

# Non-linear regime of atomic arrays at low drive intensity: controlled generation of multiple subradiant excitations via a multi-photon resonance

Orazio Scarlatella and Nigel R. Cooper

*T.C.M. Group, Cavendish Laboratory, University of Cambridge, J.J. Thomson Avenue, Cambridge CB3 0HE, United Kingdom*

Atomic arrays have emerged as an interesting light-matter platform displaying strong and controllable collective effects. In subwavelength regimes, they are characterized by a manifold of subradiant eigenstates, which can host rich quantum many-body physics and might be useful for applications. Nevertheless, their controlled excitation by a weak coherent drive is prevented by their subradiant nature. While this is true at a linear level, and although the weak-drive regime has been often described using linear theories, we point out that this regime is instead strongly non-linear for regular arrays. Using a dynamical mean-field theory (DMFT) approach, we show that by driving weakly a non-linear two-particle resonance, a steady-state with a controlled population of subradiant modes can be obtained. This features a non-zero density of interacting subradiant excitations, displaying multi-mode squeezing correlations and long-range correlations that survive many-body heating effects, even at non-zero drive intensities.

Recent advances in creating and manipulating atomic ensembles in regular geometries [1–3] have opened new avenues in controlling their collective effects [4], and important emerging applications in quantum information processing and optics [5–8]. When the inter-atomic distance becomes small enough to be comparable with the wavelength of the relevant atomic transition, the resulting dipolar interactions become strong, leading to collective effects such as superradiance and subradiance [9, 10] and Lamb shifts [11, 12]. This subwavelength regime of atomic arrays is now within experimental reach [13, 14].

In particular, subradiant states in atomic arrays have drawn increasing attention. This is the case in view of their possible applications, for example for photon storage [7, 15–21] and for quantum metrology [22–24]. Additionally, because the subradiant manifold realizes a rich open quantum many-body problem, which might host interesting phases and emergent phenomena, such as multi-particle states with a fermionic character [17, 25].

Despite their interest, subradiant states are difficult to excite, as by definition they have a very small linear coupling with far-field driving fields [17, 26, 27]. Several schemes have been proposed, exploiting geometric control [26], phase imprinting protocols [27, 28], Zeeman splittings [7, 16], spatially-modulated detunings [20], or additional Rydberg states [21]. However, these require additional (often near-field) experimental control, and can only manipulate single-particle subradiant states.

A natural route to prepare multi-particle subradiant states is to exploit the non-linearities of the atoms [19, 25, 29, 30]. While an incoherent excitation might be achieved by a strong coherent drive [19, 30], at weak drive intensities, where a controlled coherent excitation is usually achieved and heating effects are contained, non-linearities are expected to be negligible and therefore also the non-linear population of subradiant states. In fact, these were argued to vanish in the limit of small drive intensity, and the quantum many-body dynamics to be effectively described by a linear theory of coupled classical oscillators, in both cases of a disordered cloud [31]

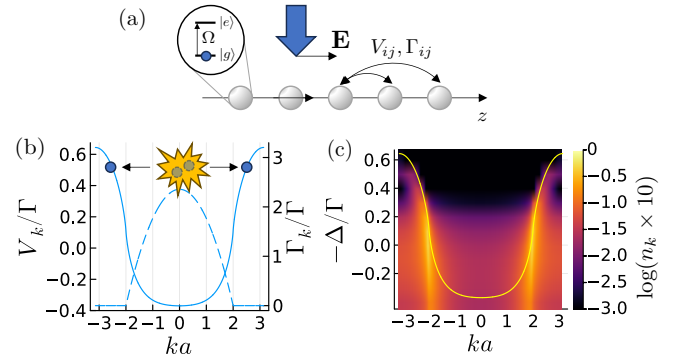


FIG. 1. (a) A 1D array of two-level atoms, driven by a classical electric field  $\mathbf{E}$  oscillating along the chain, and interacting via dipole-dipole interactions  $V_{ij}$  and subject to collective dissipation  $\Gamma_{ij}$ . (b) The dispersion relation  $V_k$  (solid line) and decay rates  $\Gamma_k$  (dashed line) as function of momentum  $k$  of collective single-particle modes, for a *subwavelength lattice spacing*,  $k_0 a = 2$ , and in the large atom number limit  $N \rightarrow \infty$ : the modes for  $|k| > k_0$  are *subradiant*, with decay rates vanishing as  $N^{-\alpha}$ . The sketch depicts a *non-linear drive* process, in which two drive photons scatter resonantly into a pair of subradiant excitations. (c) Number of steady state excitations  $n_k = \langle \sigma_k^+ \sigma_k^- \rangle$  (color code) calculated in DMFT/NCA for  $N \rightarrow \infty$ , as a function of momentum and drive detuning  $\Delta$ , for a drive strength  $\Omega/\Gamma = 0.8$ , and same lattice spacing as in (b). It shows that the subradiant modes can be controllably populated (the modes dispersion  $V_k$  is superimposed in yellow).

and regular arrays [32–34]. This effective theory was in fact extensively used in this regime [35–41]. On the other hand, in the case of arrays, it was also noticed that numerical methods tend to perform poorly down to surprisingly weak drive intensities [39].

In this paper we show that, instead, in the case of regular arrays, subradiant states can be non-linearly excited with a very weak coherent drive, with an intensity which decreases with the inverse atom number and vanishes in the large-atom-number limit. A linear approximation is

therefore inadequate and an appropriate non-linear description is needed. This observation opens up opportunities to prepare strongly-correlated driven-dissipative many-body states.

We compute such a steady state using a dynamical mean-field theory (DMFT), which has previously only been applied at strong drive intensities for which the steady-state is a trivial infinite temperature state (albeit with an interesting fluorescence spectrum) [42]. We show that, by applying a weak far-field drive resonant with a non-linear two-particle process, a steady state with a controlled population of entangled subradiant modes can be obtained. This features a finite density of multiple, interacting subradiant excitations, going well beyond a linear-response regime [31–34]. We also find that this state displays correlations well surviving many-body heating effects at finite drive intensities, including long-range correlations and multi-mode squeezing correlations, relevant for quantum computing, communication and sensing applications [43–45].

*Model.* We consider a large number  $N$  of two-level atoms ordered in a periodic array, for simplicity in a one-dimensional (1D) geometry, as illustrated in Fig. 1 (a). The atoms are illuminated with a uniform plane wave, and are coupled to the free-space electromagnetic vacuum, giving rise both to coherent dipole-dipole interactions and collective dissipation. The system can be described by the Markovian master equation [46]:

$$\dot{\rho} = -\frac{i}{\hbar}[H, \rho] + \mathcal{D}[\rho] \quad (1)$$

$$H = \frac{\hbar\Delta}{2} \sum_i^N \sigma_i^z + \frac{\hbar\Omega}{2} \sum_i^N \sigma_i^x + \sum_{i \neq j}^N \hbar V_{ij} \sigma_i^+ \sigma_j^-, \quad (2)$$

$$\mathcal{D}[\rho] = \frac{1}{2} \sum_{i,j} \Gamma_{ij} (2\sigma_i^- \rho \sigma_j^+ - \sigma_i^+ \sigma_j^- \rho - \rho \sigma_i^+ \sigma_j^-). \quad (3)$$

Here  $\sigma_l^\alpha$  with  $\alpha = x, y$  or  $z$  are the Pauli matrices on site  $l$  and  $\sigma_l^\pm = \sigma_l^x \pm i\sigma_l^y$  the raising and lowering operators;  $\Delta = \omega_0 - \omega_d$  is the detuning of the driving field, with wavevector perpendicular to the array, from the two-level transition energy  $\omega_0$  and  $\Omega = 2\mathbf{d} \cdot \mathbf{E}/\hbar$  is the Rabi coupling given by the vector of transition dipole moments  $\mathbf{d}$  and the driving electric field vector  $\mathbf{E}$ . The latter is assumed parallel to the array, corresponding to the couplings

$$V_{il} = -\frac{3\Gamma}{2} \left[ \frac{\sin k_0 r_{il}}{(k_0 r_{il})^2} + \frac{\cos k_0 r_{il}}{(k_0 r_{il})^3} \right], \quad (4)$$

$$\Gamma_{il} = 3\Gamma \left[ -\frac{\cos k_0 r_{il}}{(k_0 r_{il})^2} + \frac{\sin k_0 r_{il}}{(k_0 r_{il})^3} \right]. \quad (5)$$

Their range and relative amplitude is controlled by the parameter  $k_0 a = 2\pi a/\lambda_0$ , the ratio between lattice spacing  $a$  and the wavelength associated with the atomic transition  $\lambda_0 = 2\pi c/\omega_0$ : decreasing  $k_0 a$  these couplings become increasingly non-local, and the coherent interac-

tions strength  $V_{ij}$  dominates over the collective dissipation  $\Gamma_{ij}$ . Hereafter, we will assume units of  $\Gamma = 1$  and  $\hbar = 1$ .

*Non-linear regime at low drive intensities.* Before discussing regular arrays, we shall first consider a generic configuration of atoms – the master equation (1) also applies to that case [46].

In general, (1) constitutes a hard non-equilibrium many-body problem, with long-range interactions and dissipation. However, in the undriven case  $\Omega = 0$  in which at most a single excitation is present, it is equivalent to a non-interacting bosonic problem, obtained by replacing the spin operators with bosonic ones  $\sigma_j^- \rightarrow b_j$  [17, 47, 48]. This can be solved exactly, in terms of eigenmodes describing collective atomic excitations, characterized by frequency shifts with respect to individual atoms  $V_\alpha$ , and collective-modes decay rates  $\Gamma_\alpha$ , labeled by  $\alpha$ . In the case of a weak coherent drive  $\Omega \neq 0$ , one may approximate (1) with an analogous non-interacting bosonic theory, as by a Holstein-Primakoff representation of the spin and assuming a small number of individual modes excitations. For example, this holds for a resonantly-driven mode, with a drive strength smaller than the mode decay rate  $\Omega \ll \Gamma_\alpha$ . In fact, a non-interacting bosonic approximation may become exact in the limit of vanishing drive intensity  $\Omega \rightarrow 0$  [31, 32].

In addition, in the subwavelength regime of an average interatomic spacing smaller than the atomic transition wavelength, strongly-subradiant modes can arise, with decay rates smaller than independent atoms  $\Gamma_\alpha \ll \Gamma$ , due to interference effects. Despite their small lifetimes, for the same reason these modes have a suppressed linear coupling with far-field driving fields, thus they cannot be significantly excited, and the non-interacting theory is often a good approximation even in their presence.

Here, we show that these conclusions change drastically, and in fact do not hold, in the case of regular arrays, something that has been overlooked in previous analyses [31–41].

In this case, the crystal momentum  $\mathbf{k}$  becomes a good quantum number (for Bravais lattices) in the limit of a large array  $N \rightarrow \infty$ , and the bosonic eigenmodes correspond to reciprocal-space modes  $b_{\mathbf{k}} = \sum_j e^{i\mathbf{k} \cdot \mathbf{r}_j} b_j / \sqrt{N}$ , with a dispersion relation and decay rates given by  $V_{\mathbf{k}}$  and  $\Gamma_{\mathbf{k}}$ , the Fourier transforms of (4) and (5), shown in Fig. 1 (b) for the 1D geometry considered – here we use this geometry as a working example, but our conclusions apply for generic drive orientations/polarizations and in 2D. A manifold of subradiant eigenmodes can be understood as arising from having an energy much smaller than that of free-space photons with the same momentum along the array, and thus not being able to decay by resonant emission of a single photon [17, 26]. From this argument, one finds that such subradiance happens for subwavelength lattice spacings  $k_0 a \leq k_0^{\max} a$ , where in 1D  $k_0^{\max} = \pi$  [17], and at large momenta  $|\mathbf{k}| > k_0$  (see Fig. 1 (b)). These subradiant modes only decay by the array boundaries (in open-boundary configurations), and

their decay rates are suppressed by the number of atoms  $\Gamma_{\mathbf{k}} \sim N^{-\alpha}$  [17]. Maximal exponents of  $\alpha = 3$  in 1D and  $\alpha = 6$  in a 2D square lattice were found [17].

Importantly, despite the weak linear coupling of these subradiant modes with a far-field drive, since in regular arrays they have a well-defined momentum apart from energy, they can be addressed by *resonant, non-linear* multi-photon processes. In the following, we consider a non-linear process in which two drive photons scatter into a pair of subradiant mode excitations. This is illustrated in panel (b) of Fig. 1 for the 1D geometry considered, which is summarized in panel (a). As the photons have zero momentum along the array and total energy  $-2\Delta$  (in the rotating frame considered), they can scatter resonantly with excitations with opposite momenta  $k$  and  $-k$  and energy  $2V_{|k|} = -2\Delta$ . One can derive an effective linear bosonic model that incorporates these non-linear processes as an effective parametric drive. To lowest order in the drive strength  $\Omega$ , this corresponds to a Hamiltonian of the form  $H_{\mathbf{k}} = \delta_{-\mathbf{k}}(a_{\mathbf{k}}^\dagger a_{\mathbf{k}} + a_{-\mathbf{k}}^\dagger a_{-\mathbf{k}}) + \tilde{\delta}_{-\mathbf{k}}(a_{\mathbf{k}}^\dagger a_{-\mathbf{k}} + a_{-\mathbf{k}}^\dagger a_{\mathbf{k}}) + \lambda_{-\mathbf{k}}(a_{\mathbf{k}}^\dagger a_{\mathbf{k}}^\dagger + a_{-\mathbf{k}}^\dagger a_{-\mathbf{k}}^\dagger + \text{hc}) + \tilde{\lambda}_{-\mathbf{k}}(a_{\mathbf{k}}^\dagger a_{-\mathbf{k}}^\dagger + \text{hc})$ , where all coefficients are independent of  $N$  and of leading order  $\Omega^2$  in the drive strength – see [49] for a microscopic derivation. To the same order, the dissipator is obtained by (1) replacing spin with bosonic variables  $\sigma^- \rightarrow b$ , and is diagonal in momentum space, with decay rates  $\Gamma_{\mathbf{k}}$ . Despite such an effectively-linear model can be derived, it develops a well-known *parametric instability* for  $\Omega \gtrsim \Gamma_{|k|}^{1/2} \sim N^{-\alpha/2}$ , accompanied by a divergence of steady-state occupations (see [49]). Therefore, for a large number of atoms  $N$ , a linear theory is only valid up to a drive strength  $\Omega \lesssim \Omega_{\text{non-lin}} \sim N^{-\alpha/2}$ , which decreases with  $N$  and vanishes in the  $N \rightarrow \infty$  limit, while a non-linear description is necessarily needed for stronger drives. Apart from being at odds with the expectation that weakly driven atomic ensembles display a linear behavior [31–41], this non-linear regime at weak drives in arrays opens up opportunities to realize strongly-correlated many-body driven-dissipative states, with pristine quantum properties.

*Correlated stationary state in DMFT.* To capture the relevant physics, we approximate the non-linear many-body problem using the dynamical mean-field theory (DMFT) developed in [42]. This allows one to compute the *homogeneous steady state* of (1) in the thermodynamic limit  $N \rightarrow \infty$  (in which the problem is non-linear, no matter how weak the drive). DMFT maps the lattice model (1) onto an effective model of a single-site, coupled to a self-consistent magnetic field and non-Markovian environment, where the latter captures genuine correlations (it improves on a Gutzwiller mean-field theory, which assumes a factorized density matrix). To solve the effective model, we use a method based on a strong-coupling expansion in the DMFT bath, truncated to lowest order – known as a non-crossing approximation (NCA) [50–52]. Since a simple fixed-point iteration scheme to solve the DMFT equations does not converge at weak drive inten-

sities, we developed new numerical methods, adapting a linear mixing scheme, and a Broyden algorithm [53] estimating their gradient [49]. Some more details on our DMFT/NCA approach are given in the Supplemental Material [49], and in [42].

At weak drive intensities  $\Omega \lesssim \Gamma$ , a selective steady-state population of the subradiant modes resonant via the two-photon resonance described (Fig. 1 (a)) is indeed captured by our DMFT approach. This is shown in Fig. 1 (c), plotting the number of excitations in a momentum mode  $n_k = \langle \sigma_k^+ \sigma_k^- \rangle$  as a function of momentum  $k$  and drive detuning, where  $\sigma_k^- = \sum_j e^{ikr_j} \sigma_j^- / \sqrt{N}$ . A delta-function contribution to the  $k = 0$  mode is not shown, and will be discussed later. Comparing with the dispersion relation (also plotted), one sees that when the subradiant modes are resonant  $-\Delta \gtrsim V_{k_0} \approx 0.1\Gamma$ , these are selectively populated. By contrast, when the radiative modes are resonant  $-\Delta \lesssim 0.1\Gamma$ , these do not get significantly populated, as their non-zero lifetimes prevent the parametric instability to occur: in this case, the instability is realized at non-zero detuning, with the modes with lowest decay rates and closest to resonance, at  $|k| \approx k_0$ . We stress that the parametric drive brings the subradiant modes into a *non-linear regime* of multiple *interacting* excitations: as discussed with the linear effective model, their number can only be bound by non-linearities. These have a *non-zero density* and therefore are far from the single-excitation regime (which has zero density for  $N \rightarrow \infty$ ): the densities are of order  $n_{\text{c,subrad}} = \sum_{|k| > k_0} \langle \sigma_k^+ \sigma_k^- \rangle_{\text{c}} / N \approx 0.05$  for a drive strength  $\Omega/\Gamma \approx 1$  (perhaps underestimated by our method). At the same time, these excitations are still subradiant, having an energy and momentum strongly mismatched with free photons [17].

In addition to achieving a controlled population of subradiant excitations, the non-linear parametric-drive process naturally creates them in entangled pairs. Nevertheless, the resulting correlations could be suppressed by many-body heating effects, and by the coupling with the environment. To assess this competition, we report the pair correlation function  $\langle \sigma_k^- \sigma_{-k}^- \rangle_{\text{c}}$  or its real-space counterpart  $\langle \sigma_i^- \sigma_j^- \rangle_{\text{c}}$  in Fig. 2 (we also looked at  $\langle \sigma_k^+ \sigma_k^- \rangle_{\text{c}}$ , but this adds no further insights thus is not shown). Here  $\langle AB \rangle_{\text{c}} \equiv \langle AB \rangle - \langle A \rangle \langle B \rangle$  is a “connected” function (subscript “c”), capturing genuine correlations (it vanishes for a factorized density matrix).

As the drive strength is decreased, Fig. 2 (a) shows that two-mode squeezing correlations are present between each pair of modes with momenta  $k$  and  $-k$ , which peak at the momenta resonant with the parametric drive. We remark that, although these correlations resemble a bosonic multi-mode squeezed state [54, 55], this is by contrast a non-linear or equivalently *non-gaussian* state, as already discussed. Correlations also acquire a long-range character in real space, as shown in Fig. 2 (b), displaying the non-local part of the Fourier transform of the same correlation function  $\langle \sigma_i^- \sigma_j^- \rangle_{\text{c}}$ . Both panels also

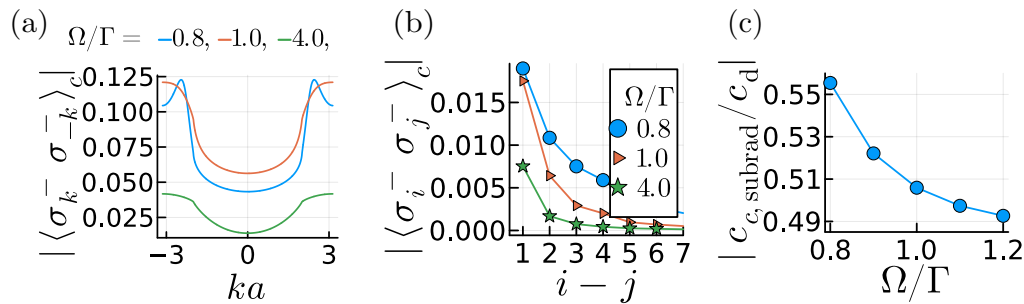


FIG. 2. Pair correlation function of the steady state in DMFT/NCA, for a fixed drive detuning  $\Delta/\Gamma = -0.4$  resonant with a pair of subradiant modes, and for the same conditions as in Fig. 1. The subscript “c” (“d”) indicates its connected (disconnected) component, describing non-linear correlations (an uncorrelated linear component). (a) The connected function as a function momentum  $k$  for different drive strengths  $\Omega$ : this shows two-mode squeezing correlations of each modes-pair with momenta  $k, -k$ . Decreasing the drive strength it becomes more sharply peaked around the resonantly-driven modes. (b) The non-local component of the same correlation function in real space, depending on lattice sites distance  $i - j$ , showing long-range correlations. Both (a) and (b) also show that correlations increase in magnitude, as the drive is decreased in the range considered, as a non-trivial interplay of reduced many-body heating effects, and reduced occupation. (c) The ratio between the connected correlation function summed over the subradiant modes  $c_{c, \text{subrad}} = \sum_{|k| > k_0} \langle \sigma_k^- \sigma_{-k}^- \rangle_c / N$  and its disconnected component  $c_d = \langle \sigma_{k=0}^- \rangle \langle \sigma_{k=0}^- \rangle / N$ , showing that the non-linear, subradiant steady-state component is way non-negligible, and increasing for decreasing drive intensities.

show a second important fact: the amplitude of these correlations increases decreasing the drive strength, in the interval considered. This results from a non-trivial interplay between decreased heating effects, and decreased number of excitations. Decreasing the drive further it is expected that a maximum is reached and then the trend inverts, as the amplitude of correlations becomes limited by the excitations density. This is not shown, as the DMFT/NCA results break down for smaller drive intensities, due to the non-crossing approximation (NCA) eventually becoming inaccurate. Therefore, we limited our analysis to an intermediate-drive regime, where the approach is well behaved. Note though that, instead, the DMFT approximation alone is in principle highly-appropriate both in the weak and large drives regimes, as discussed in [49]. Even with these limitations, our results show that multi-mode squeezing and long range correlations survive many-body heating effects at finite drive strengths and despite the coupling to the environment, demonstrating that strongly quantum-correlated many-body states can be achieved.

Although the multi-photon process considered is by definition non-linear, there is also an uncorrelated, linear component to the steady-state. This is due to the linear coupling of the driving field with the zero momentum  $k = 0$  collective mode (for our geometry), giving rise to a non-zero average  $\langle \sigma_j^- \rangle$ . It is the only component that is captured by a linear bosonic theory with a coherent drive (rather than an effective parametric one), and one might wonder if this is the dominant contribution, and if non-linearities could be neglected altogether. An estimate of the relative importance of the non-linear and linear components is given by the ratio  $W(A) = -c_{c,A}/c_d$ , between the connected pair correlation function summed

over a momentum region  $A$ ,  $c_{c,A} = \sum_{k \in A} \langle \sigma_k^- \sigma_{-k}^- \rangle_c / N$ , and the sum over the disconnected component (a delta function at  $k = 0$ ),  $c_d = \langle \sigma_{k=0}^- \rangle \langle \sigma_{k=0}^- \rangle / N$ . Note that if  $A$  is the entire Brillouin zone, then the numerator is rigidly related to the denominator by a sum rule  $-c_c = \langle \sigma_j^- \rangle \langle \sigma_j^- \rangle = c_d$  and the ratio is always  $W = 1$  (this is because  $\langle \sigma_i^- \sigma_i^- \rangle = 0$ ) – remarkably such rule is respected in DMFT/NCA. Note that this is independent of the state at hand, so it is not yet a measure of how non-linear this is. It shows that  $W(A)$  defines a spectral weight of the non-linear modes correlations, whose sum over all momentum partitions is independent of drive intensity, i.e. it is a normalized spectral weight. For  $A$  a subset of the Brillouin zone, a weight  $W(A)$  of order one is a genuine indication that its non-linear contribution is comparable with the linear component  $c_d$ . This is indeed the case if we consider the subradiant region  $|k| > k_0$  in our problem, as shown in Fig. 2 (c). Therefore, such subradiant contribution is non-negligible, and actually its weight is found to increase as drive intensity is decreased. On the other hand, we also note that the linear uncorrelated component is superradiant and would be quickly dissipated by switching the drive off.

Finally, while here we focused on the steady state density matrix, in the Supplemental Material [49] we also show that non-linearities play an important role in dynamical local correlation functions, in the weak-drive-intensity limit. We also note that, while a Gutzwiller mean-field approximation predicts instabilities of the uniform steady-state solutions and non-uniform phases [37], these only occur at much smaller lattice spacings than considered here, for which our DMFT/NCA approach does not converge. Instead, for the spacings considered or larger, both the DMFT/NCA steady state and the

mean-field one are always stable, as confirmed by a linear stability analysis (see [49]).

*Conclusions* – We demonstrated that the weak-drive-intensity regime of large subwavelength atomic arrays is non-linear, due to a large non-linear response of subradiant modes, something that was overlooked in previous works [31–41]. This opens up opportunities to prepare strongly-correlated driven-dissipative many-body states. Using a dynamical mean-field theory (DMFT), we showed that by a weak coherent far-field drive of a two-particle resonance, a steady-state with a controlled population of multiple, non-zero-density, and interacting subradiant excitations can be generated. This features multi-mode squeezing correlations (although is a non-gaussian state) and long-range correlations, surviving many-body heating effects, even at finite drive intensities. Experiments might find this preparation schemes appealing, requiring only a uniform coherent far-field drive, which is easily accessible. These are getting close

to the subwavelength regime required, despite this remains their current challenge [13, 14, 56, 57].

An interesting future direction of this work would be to go beyond the non-crossing approximation used, to further explore the many-body physics of the model at weaker drive intensities and smaller lattice spacings within DMFT.

*Acknowledgements* – We thank Mike Gunn for insightful discussions. This work was supported by the Engineering and Physical Sciences Research Council and Science and Technology Facilities Council [grant number EP/W005484], and a Simons Investigator Award [Grant No. 511029]. For the purpose of open access, the authors has applied a creative commons attribution (CC BY) licence to any author accepted manuscript version arising.

The data (code) to reproduce the results of the manuscript will be provided by the author under request.

- 
- [1] M. Endres, H. Bernien, A. Keesling, H. Levine, E. R. Anschuetz, A. Krajenbrink, C. Senko, V. Vuletic, M. Greiner, and M. D. Lukin, Atom-by-atom assembly of defect-free one-dimensional cold atom arrays, *Science* **354**, 1024 (2016).
- [2] D. Barredo, S. de Léséleuc, V. Lienhard, T. Lahaye, and A. Browaeys, An atom-by-atom assembler of defect-free arbitrary two-dimensional atomic arrays, *Science* **354**, 1021 (2016).
- [3] D. Barredo, V. Lienhard, S. de Léséleuc, T. Lahaye, and A. Browaeys, Synthetic three-dimensional atomic structures assembled atom by atom, *Nature* **561**, 79 (2018).
- [4] J. Ruostekoski, Cooperative quantum-optical planar arrays of atoms, *Physical Review A* **108**, 030101 (2023).
- [5] T. L. Patti, D. S. Wild, E. Shahmoon, M. D. Lukin, and S. F. Yelin, Controlling Interactions between Quantum Emitters Using Atom Arrays, *Physical Review Letters* **126**, 223602 (2021).
- [6] A. S. Solntsev, G. S. Agarwal, and Y. S. Kivshar, Metasurfaces for quantum photonics, *Nature Photonics* **15**, 327 (2021).
- [7] K. E. Ballantine and J. Ruostekoski, Quantum Single-Photon Control, Storage, and Entanglement Generation with Planar Atomic Arrays, *PRX Quantum* **2**, 040362 (2021).
- [8] R. Bekenstein, I. Pikovski, H. Pichler, E. Shahmoon, S. F. Yelin, and M. D. Lukin, Quantum metasurfaces with atom arrays, *Nature Physics* **16**, 676 (2020).
- [9] R. H. Dicke, Coherence in Spontaneous Radiation Processes, *Physical Review* **93**, 99 (1954).
- [10] M. Gross and S. Haroche, Superradiance: An essay on the theory of collective spontaneous emission, *Physics Reports* **93**, 301 (1982).
- [11] R. Friedberg, S. R. Hartmann, and J. T. Manassah, Frequency shifts in emission and absorption by resonant systems of two-level atoms, *Physics Reports* **7**, 101 (1973).
- [12] J. Keaveney, A. Sargsyan, U. Krohn, I. G. Hughes, D. Sarkisyan, and C. S. Adams, Cooperative Lamb Shift in an Atomic Vapor Layer of Nanometer Thickness, *Physical Review Letters* **108**, 173601 (2012).
- [13] K. Srakaew, P. Weckesser, S. Hollerith, D. Wei, D. Adler, I. Bloch, and J. Zeiher, A subwavelength atomic array switched by a single Rydberg atom, *Nature Physics* **19**, 714 (2023).
- [14] J. Rui, D. Wei, A. Rubio-Abadal, S. Hollerith, J. Zeiher, D. M. Stamper-Kurn, C. Gross, and I. Bloch, A subradiant optical mirror formed by a single structured atomic layer, *Nature* **583**, 369 (2020).
- [15] D. Plankensteiner, L. Ostermann, H. Ritsch, and C. Genes, Selective protected state preparation of coupled dissipative quantum emitters, *Scientific Reports* **5**, 16231 (2015).
- [16] G. Facchinetti, S. D. Jenkins, and J. Ruostekoski, Storing Light with Subradiant Correlations in Arrays of Atoms, *Physical Review Letters* **117**, 243601 (2016).
- [17] A. Asenjo-Garcia, M. Moreno-Cardoner, A. Albrecht, H. J. Kimble, and D. E. Chang, Exponential Improvement in Photon Storage Fidelities Using Subradiance and “Selective Radiance” in Atomic Arrays, *Physical Review X* **7**, 031024 (2017).
- [18] J. A. Needham, I. Lesanovsky, and B. Olmos, Subradiance-protected excitation transport, *New Journal of Physics* **21**, 073061 (2019).
- [19] G. Ferioli, A. Glicenstein, L. Henriët, I. Ferrier-Barbut, and A. Browaeys, Storage and Release of Subradiant Excitations in a Dense Atomic Cloud, *Physical Review X* **11**, 021031 (2021).
- [20] O. Rubies-Bigorda, V. Walther, T. L. Patti, and S. F. Yelin, Photon control and coherent interactions via lattice dark states in atomic arrays, *Physical Review Research* **4**, 013110 (2022).
- [21] M. Cech, I. Lesanovsky, and B. Olmos, Dispersionless subradiant photon storage in one-dimensional emitter chains, *Physical Review A* **108**, L051702 (2023).
- [22] L. Ostermann, H. Ritsch, and C. Genes, Protected State Enhanced Quantum Metrology with Interacting Two-Level Ensembles, *Physical Review Letters* **111**, 123601 (2013).

- [23] G. Facchinetti and J. Ruostekoski, Interaction of light with planar lattices of atoms: Reflection, transmission, and cooperative magnetometry, *Physical Review A* **97**, 023833 (2018).
- [24] C. Qu and A. M. Rey, Spin squeezing and many-body dipolar dynamics in optical lattice clocks, *Physical Review A* **100**, 041602 (2019).
- [25] L. Henriët, J. S. Douglas, D. E. Chang, and A. Albrecht, Critical open-system dynamics in a one-dimensional optical-lattice clock, *Physical Review A* **99**, 023802 (2019).
- [26] Y. He, L. Ji, Y. Wang, L. Qiu, J. Zhao, Y. Ma, X. Huang, S. Wu, and D. E. Chang, Geometric Control of Collective Spontaneous Emission, *Physical Review Letters* **125**, 213602 (2020).
- [27] M. Zanner, T. Orell, C. M. F. Schneider, R. Albert, S. Oleschko, M. L. Juan, M. Silveri, and G. Kirchmair, Coherent control of a multi-qubit dark state in waveguide quantum electrodynamics, *Nature Physics* **18**, 538 (2022).
- [28] H. H. Jen, M.-S. Chang, and Y.-C. Chen, Cooperative single-photon subradiant states, *Physical Review A* **94**, 013803 (2016).
- [29] O. Rubies-Bigorda, S. Ostermann, and S. F. Yelin, Dynamic population of multiexcitation subradiant states in incoherently excited atomic arrays, *Physical Review A* **107**, L051701 (2023).
- [30] S. Ostermann, O. Rubies-Bigorda, V. Zhang, and S. F. Yelin, Breakdown of steady-state superradiance in extended driven atomic arrays, *Physical Review Research* **6**, 023206 (2024).
- [31] J. Ruostekoski and J. Javanainen, Quantum field theory of cooperative atom response: Low light intensity, *Physical Review A* **55**, 513 (1997).
- [32] J. Javanainen, One-dimensional modeling of light propagation in dense and degenerate samples, *Physical Review A* **59**, 649 (1999).
- [33] M. D. Lee, S. D. Jenkins, and J. Ruostekoski, Stochastic methods for light propagation and recurrent scattering in saturated and nonsaturated atomic ensembles, *Physical Review A* **93**, 063803 (2016).
- [34] L. A. Williamson and J. Ruostekoski, Optical response of atom chains beyond the limit of low light intensity: The validity of the linear classical oscillator model, *Physical Review Research* **2**, 023273 (2020).
- [35] R. J. Bettles, S. A. Gardiner, and C. S. Adams, Cooperative ordering in lattices of interacting two-level dipoles, *Physical Review A* **92**, 063822 (2015).
- [36] R. J. Bettles, S. A. Gardiner, and C. S. Adams, Enhanced Optical Cross Section via Collective Coupling of Atomic Dipoles in a 2D Array, *Physical Review Letters* **116**, 103602 (2016).
- [37] C. D. Parmee and N. R. Cooper, Phases of driven two-level systems with nonlocal dissipation, *Physical Review A* **97**, 053616 (2018).
- [38] R. T. Sutherland and F. Robicheaux, Collective dipole-dipole interactions in an atomic array, *Physical Review A* **94**, 013847 (2016).
- [39] F. Robicheaux and D. A. Suresh, Beyond lowest order mean-field theory for light interacting with atom arrays, *Physical Review A* **104**, 023702 (2021).
- [40] A. Glicenstein, G. Ferioli, N. Šibalić, L. Brossard, I. Ferrier-Barbut, and A. Browaeys, Collective Shift in Resonant Light Scattering by a One-Dimensional Atomic Chain, *Physical Review Letters* **124**, 253602 (2020).
- [41] W. Guerin, M. O. Araújo, and R. Kaiser, Subradiance in a Large Cloud of Cold Atoms, *Physical Review Letters* **116**, 083601 (2016).
- [42] O. Scarlatella and N. R. Cooper, Fate of the Mollow triplet in strongly coupled atomic arrays, *Physical Review A* **110**, L041305 (2024).
- [43] U. L. Andersen, T. Gehring, C. Marquardt, and G. Leuchs, 30 years of squeezed light generation, *Physica Scripta* **91**, 053001 (2016).
- [44] M. V. Chekhova, G. Leuchs, and M. Żukowski, Bright squeezed vacuum: Entanglement of macroscopic light beams, *Optics Communications Macroscopic Quantumness: Theory and Applications in Optical Sciences*, **337**, 27 (2015).
- [45] M. D. Reid, P. D. Drummond, W. P. Bowen, E. G. Cavalcanti, P. K. Lam, H. A. Bachor, U. L. Andersen, and G. Leuchs, Colloquium: The Einstein-Podolsky-Rosen paradox: From concepts to applications, *Reviews of Modern Physics* **81**, 1727 (2009).
- [46] R. H. Lehmann, Radiation from an N-Atom System. I. General Formalism, *Physical Review A* **2**, 883 (1970).
- [47] D. Porras and J. I. Cirac, Collective generation of quantum states of light by entangled atoms, *Physical Review A* **78**, 053816 (2008).
- [48] A. A. Svidzinsky, J.-T. Chang, and M. O. Scully, Cooperative spontaneous emission of N atoms: Many-body eigenstates, the effect of virtual Lamb shift processes, and analogy with radiation of N classical oscillators, *Physical Review A* **81**, 053821 (2010).
- [49] See supplemental material [url will be inserted by publisher].
- [50] M. Schiro and O. Scarlatella, Quantum impurity models coupled to Markovian and non-Markovian baths, *The Journal of Chemical Physics* **151**, 044102 (2019).
- [51] O. Scarlatella, A. A. Clerk, R. Fazio, and M. Schirò, Dynamical Mean-Field Theory for Markovian Open Quantum Many-Body Systems, *Physical Review X* **11**, 031018 (2021).
- [52] O. Scarlatella and M. Schirò, Self-consistent dynamical maps for open quantum systems, *SciPost Physics* **16**, 026 (2024).
- [53] R. Žitko, Convergence acceleration and stabilization of dynamical mean-field theory calculations, *Physical Review B* **80**, 125125 (2009).
- [54] D. F. Walls and G. J. Milburn, *Quantum Optics* (Springer Science & Business Media, 2007).
- [55] M. O. Scully and M. S. Zubairy, *Quantum Optics* (Cambridge University Press, Cambridge, 1997).
- [56] B. Olmos, D. Yu, Y. Singh, F. Schreck, K. Bongs, and I. Lesanovsky, Long-Range Interacting Many-Body Systems with Alkaline-Earth-Metal Atoms, *Physical Review Letters* **110**, 143602 (2013).
- [57] J. P. Covey, A. Sipahigil, S. Szoke, N. Sinclair, M. Endres, and O. Painter, Telecom-Band Quantum Optics with Ytterbium Atoms and Silicon Nanophotonics, *Physical Review Applied* **11**, 034044 (2019).
- [58] A. Altland and B. Simons, *Condensed Matter Field Theory*, 2nd ed. (Cambridge University Press, 2012).
- [59] M. Ganahl, M. Aichhorn, H. G. Evertz, P. Thunström, K. Held, and F. Verstraete, Efficient DMFT impurity solver using real-time dynamics with matrix product states, *Physical Review B* **92**, 155132 (2015).

- [60] A. Georges, G. Kotliar, W. Krauth, and M. J. Rozenberg, Dynamical mean-field theory of strongly correlated fermion systems and the limit of infinite dimensions, *Reviews of Modern Physics* **68**, 13 (1996).
- [61] H. Aoki, N. Tsuji, M. Eckstein, M. Kollar, T. Oka, and P. Werner, Nonequilibrium dynamical mean-field theory and its applications, *Reviews of Modern Physics* **86**, 779 (2014).

**SUPPLEMENTAL MATERIAL FOR:  
“NON-LINEAR REGIME OF ATOMIC ARRAYS AT LOW DRIVE INTENSITY:  
CONTROLLED GENERATION OF MULTIPLE SUBRADIANT EXCITATIONS VIA A MULTI-PHOTON  
RESONANCE”**

This Supplemental Material is organized as follows. In Sec. A we derive an effective linear theory, of parametrically-driven bosons, from the non-linear driving scheme considered in the main text. An even more naive effective linear theory of linearly driven bosons, rather than parametrically driven, is discussed in Sec. B, and its problems in describing the relaxation of time-dependent correlation functions is pointed out. In Sec. C we discuss the main equations of our DMFT approach, in Sec. D the numerical schemes to solve them, and in Sec. E two exact limits of DMFT. In Sec. F we study the linear stability of the DMFT solution.

**Appendix A: Effective linear theory of  
parametrically-driven bosons**

The usual formulation of the Holstein-Primakoff transformation is

$$\begin{aligned}\sigma_i^- &= a_i^\dagger \left(2S - a_i^\dagger a_i\right)^{1/2}, \\ \sigma_i^+ &= \left(2S - a_i^\dagger a_i\right)^{1/2} a_i, \\ \sigma_i^z &= 2(S - a_i^\dagger a_i).\end{aligned}$$

For  $S = 1/2$ , this preserves the  $SU(2)$  commutation relations:

$$[\sigma_i^z, \sigma_j^\pm] = \pm \delta_{ij} 2\sigma_i^\pm, \quad [\sigma_i^+, \sigma_j^-] = \delta_{ij} \sigma_i^z.$$

That formulation is around the maximum weight state, while here we need one around the lowest-weight state. This is achieved by

$$\begin{aligned}\sigma_i^- &= \left(2S - a_i^\dagger a_i\right)^{1/2} a_i, \\ \sigma_i^+ &= a_i^\dagger \left(2S - a_i^\dagger a_i\right)^{1/2}, \\ \sigma_i^z &= 2(a_i^\dagger a_i - S).\end{aligned}$$

With respect to the maximum-weight transformation, this corresponds to  $\sigma^z \rightarrow -\sigma^z$  and  $\sigma^- \rightarrow \sigma^+$ , a rotation that leaves the commutation relations unchanged.

Expanding the square root to first order one gets  $\sigma_i^+ = (a_i^\dagger - a_i^\dagger a_i^\dagger a_i/2)$  and  $\sigma_i^z = (-1 + 2a_i^\dagger a_i)$ , and for the Hamiltonian

$$\begin{aligned}H &= \frac{\Delta}{2} \sum_i \sigma_i^z + \frac{\Omega}{2} \sum_i \sigma_i^x + \sum_{i \neq j} V_{ij} \sigma_i^+ \sigma_j^- \\ &\approx \sum_i \Delta \left(-\frac{1}{2} + a_i^\dagger a_i\right) + \sum_{i \neq j} V_{ij} a_i^\dagger a_j + \sum_i \frac{\Omega}{2} (a_i + a_i^\dagger) \\ &\quad - \sum_i \frac{\Omega}{4} (a_i^\dagger a_i^\dagger a_i + \text{hc}) - \sum_{i \neq j} \frac{V_{ij}}{2} (a_i^\dagger a_i^\dagger a_i a_j + \text{hc}) + \dots\end{aligned}\tag{A1}$$

As we want to capture a parametric drive process in which two drive photons with momenta  $k = 0$  scatter resonantly into atomic excitations with momenta  $k$  and  $-k$ , we assume periodic boundary conditions, and transform to momentum space  $a_{\mathbf{k}} = \sum_j e^{i\mathbf{k}\cdot\mathbf{r}_j} a_j / \sqrt{N}$ :

$$\begin{aligned}H &= \sum_k (\Delta + V_k) a_k^\dagger a_k + \frac{\sqrt{N}\Omega}{2} (a_{k=0} + a_{k=0}^\dagger) \\ &\quad - \sum_{kq} \frac{\Omega}{4\sqrt{N}} (a_{k-q}^\dagger a_q^\dagger a_k + \text{hc}) \\ &\quad - \sum_{kqp} \frac{V_k}{2N} (a_{q-k-p}^\dagger a_p^\dagger a_q a_k + \text{hc}) + \dots\end{aligned}\tag{A2}$$

As the  $k = 0$  mode is linearly coupled to a coherent drive, we solve this independently from the other modes, yielding

$$\alpha_0 = \langle a_{k=0} \rangle = -\sqrt{N}\Omega / [(\Delta + V_{k=0}) - i\Gamma_{k=0}] = \sqrt{N}\Omega \tilde{\alpha}_0\tag{A3}$$

Then, as this mode is in a coherent state, with macroscopic occupation  $|\alpha_0|^2 \sim N$ , we replace  $a_{k=0} \rightarrow \alpha_0$  such as to generate an effective quadratic Hamiltonian for the other modes.

Before writing the Hamiltonian for these modes, we perform a power counting in  $N$  and  $\Omega$ . We assume a scaling  $\Omega \sim N^{-\alpha/2}$  for the latter, which we will verify a posteriori. For this purpose, consider the real-space Hamiltonian:

- when transforming it to momentum space, each field  $a_j$  introduces a  $1/\sqrt{N}$  factor ( $a_j = \sum_{\mathbf{k}} e^{-i\mathbf{k}\cdot\mathbf{r}_j} a_{\mathbf{k}} / \sqrt{N}$ )
- translation invariance leads to a factor of  $N$  for each term in the Hamiltonian:  $\sum_j e^{i\mathbf{k}\cdot\mathbf{r}_j} = \delta_{\mathbf{k}} N$
- each zero-momentum field imposed gives a contribution  $\alpha_0 = \sqrt{N}\Omega \tilde{\alpha}_0$

Then, the term  $\propto V$ , being particle-conserving, generates even powers of the bosonic fields  $a^{2n}$ , leading to an overall scaling for each of them

$$\sum_j \sum_{i-j} V_{ij} \sigma_i^+ \sigma_j^- \rightarrow N \frac{1}{(\sqrt{N})^{2n}} (\Omega \sqrt{N})^{2n-2} = \Omega^{2n-2}.$$

Instead the particle-non-conserving term  $\propto \Omega$  generates odd powers  $a^{2n-1}$ , yielding

$$\Omega \sum_j \sigma_j^x \rightarrow \Omega N \frac{1}{(\sqrt{N})^{2n-1}} (\Omega \sqrt{N})^{2n-3} = \Omega^{2n-2}.$$

Importantly, both kind of terms do not depend on  $N$  explicitly. Also, one can keep only the lowest-order terms



in  $\Omega$ , of order  $\Omega^2$ . For  $\Omega \sim N^{-\alpha/2}$ , these are order  $N^{-\alpha}$ . Similar calculations for the dissipator, considering that  $\Gamma \sim N^{-\alpha}$ , lead to

$$\begin{aligned} \mathcal{D} &\rightarrow \Gamma N \left( \frac{1}{(\sqrt{N})^2} + \frac{(\Omega\sqrt{N})^2}{(\sqrt{N})^4} + \dots \right) \\ &\sim \Gamma (1 + \Omega^2 + \dots) \sim N^{-\alpha} + N^{-2\alpha} + \dots \end{aligned}$$

The first term is the leading one, of the same order of the

leading-order Hamiltonian terms. Therefore the effective bosonic dissipator is simply obtained by replacing spins with bosons:  $\sigma_{\mathbf{k}}^- \rightarrow a_{\mathbf{k}}$ .

The effective bosonic Hamiltonian is then a generalized parametric-drive Hamiltonian, containing both single-mode and two-modes drive terms, as well as number conserving terms. This reads

$$\begin{aligned} H^{k>0} &\approx \sum_{k>0} \left( a_k^\dagger a_k + a_{-k}^\dagger a_{-k} \right) \left[ \Delta + V_k - \Omega^2 \left( (\text{Re}\tilde{\alpha}_0)^2 + 2|\tilde{\alpha}_0|^2 V_0 \right) \right] \\ &+ \sum_{k>0} \left( a_k^\dagger a_{-k} + a_{-k}^\dagger a_k \right) \left( -2\Omega^2 |\tilde{\alpha}_0|^2 V_k \right) \\ &+ \sum_{k>0} \left[ \left( a_k^\dagger a_k^\dagger + a_{-k}^\dagger a_{-k}^\dagger \right) \left( -\Omega^2 \frac{V_k}{2} \tilde{\alpha}_0^2 \right) + \text{hc} \right] \\ &+ \sum_{k>0} \left[ \left( a_{-k}^\dagger a_k^\dagger + a_k^\dagger a_{-k}^\dagger \right) \left( -\frac{\Omega^2}{4} \tilde{\alpha}_0^2 - \Omega^2 \frac{V_0}{2} \tilde{\alpha}_0^2 \right) + \text{hc} \right] \end{aligned} \quad (\text{A4})$$

On resonance  $\Delta = -V_k$ , all terms are of leading order  $\Omega^2$ .

Each couple of modes with momentum  $k, -k$  is independent from each other, and for a single couple the Hamiltonian takes the form  $H = \delta(a^\dagger a + b^\dagger b) + \tilde{\delta}(a^\dagger b + b^\dagger a) + \lambda(a^\dagger a^\dagger + b^\dagger b^\dagger + \text{hc}) + \tilde{\lambda}(a^\dagger b^\dagger + \text{hc})$ . For  $\tilde{\delta}, \tilde{\Lambda} = 0$  ( $\delta, \Lambda = 0$ ) a dynamical instability occurs for a drive  $|\lambda|^2 > \delta^2 + \Gamma^2$  ( $|\tilde{\lambda}|^2 > \tilde{\delta}^2 + \Gamma^2$ ). In these cases, as  $\Gamma \sim N^{-\alpha/2}$  and  $\lambda, \delta, \tilde{\lambda}, \tilde{\delta} \sim \Omega^2$ , an instability occurs for

$$\Omega \lesssim N^{-\alpha/2} \quad (\text{A5})$$

This corresponds to the scaling guessed a priori, for which we showed that the discarded terms are subleading. For completeness, we check that this also holds in the general case. In this case, one can consider the quadratic Green's function of the Keldysh-Nambu vector  $(a_+^\dagger b_+^\dagger a_+ b_+ a_-^\dagger b_-^\dagger a_- b_-)$ , where  $+$  and  $-$  are Keldysh indices. Its inverse, in frequency domain and for  $\omega = 0$ , is given by

$$G^{-1}(\omega = 0) = \begin{pmatrix} -\delta - i\Gamma & -\tilde{\delta} & \lambda & \tilde{\lambda} & 0 & 0 & 0 & 0 \\ -\tilde{\delta} & -\delta - i\Gamma & \tilde{\lambda} & \lambda & 0 & 0 & 0 & 0 \\ \lambda^* & \tilde{\lambda}^* & -\delta - i\Gamma & -\tilde{\delta} & 0 & 0 & 2i\Gamma & 0 \\ \tilde{\lambda}^* & \lambda^* & -\tilde{\delta} & -\delta - i\Gamma & 0 & 0 & 0 & 2i\Gamma \\ 2i\Gamma & 0 & 0 & 0 & \delta - i\Gamma & \tilde{\delta} & -\lambda & -\tilde{\lambda} \\ 0 & 2i\Gamma & 0 & 0 & \tilde{\delta} & \delta - i\Gamma & -\tilde{\lambda} & -\lambda \\ 0 & 0 & 0 & 0 & -\lambda^* & -\tilde{\lambda}^* & \delta - i\Gamma & \tilde{\delta} \\ 0 & 0 & 0 & 0 & -\tilde{\lambda}^* & -\lambda^* & \tilde{\delta} & \delta - i\Gamma \end{pmatrix}$$

Dynamical instabilities are then determined by the poles of  $G$ , which correspond to the zeros the determinant

$$\det G^{-1}(\omega = 0) = \left( \Gamma^2 - |\lambda - \tilde{\lambda}|^2 + (\delta - \tilde{\delta})^2 \right)^2 \left( \Gamma^2 - |\lambda + \tilde{\lambda}|^2 + (\delta + \tilde{\delta})^2 \right)^2$$

In the general case, inserting  $\Gamma \sim N^{-\alpha/2}$  and  $\lambda, \delta, \tilde{\lambda}, \tilde{\delta} \sim \Omega^2$  in the determinant, both factors lead to the same instability condition than for the well-known specific cases  $\tilde{\delta}, \tilde{\Lambda} = 0$  ( $\delta, \Lambda = 0$ ).

### Appendix B: Effective linear theory of coherently-driven bosons: relaxation of correlation functions

When the atoms are weakly excited, one can neglect their non-linearities all together, and replace the spins

with bosonic operators  $\sigma_j^- \rightarrow b_j$ , according to a Holstein-Primakoff approximation [47] (see also A). The model

(1) then reduces to one of non-interacting bosons that is exactly solvable (this is also known as coupled-dipole model). This approximation is usually valid at sufficiently weak drive intensities  $\Omega \ll \Gamma_k$ , but fails in the presence of subradiant modes and for a large number of atoms  $N$ , as discussed in the main text.

In the thermodynamic limit  $N \rightarrow \infty$ , the non-interacting model is diagonal in reciprocal space. The steady-state, single-particle Green's functions are easily obtained in a Keldysh formalism. In the limit of vanishing drive  $\Omega \rightarrow 0$  the problem becomes diagonal in Nambu space and one gets in the basis of classical and quantum fields for the inverse Green's function

$$\chi_{11}^{-1}(k, \omega) = \begin{pmatrix} 0 & \omega - \Delta - V_k - \frac{i}{2}\Gamma_k \\ \omega - \Delta - V_k + \frac{i}{2}\Gamma_k & i\Gamma_k \end{pmatrix} \quad (\text{B1})$$

In the presence of subradiant modes with zero damping, in the subwavelength regime, whether local correlation functions can relax to a steady state is a non-trivial question. These, probe the relaxation of a local excitation created in the steady state, which therefore excites all momentum modes and whose long-time dynamics is dominated by the non-radiative modes. Local correlation functions are obtained by a matrix inversion of (B1) and a sum over momentum  $\chi_{11} = \sum_k \chi_{11}(k, \omega)$ . We consider for example the Keldysh component, corresponding to the top-left entry of the matrix, defined as  $i\chi_{11}^K(\tau) = \lim_{t \rightarrow \infty} \langle \{ \sigma_i^-(t + \tau), \sigma_i^+(t) \} \rangle - \langle \sigma_i^-(t + \tau) \rangle \langle \sigma_i^+(t) \rangle$ .

Even in a non-interacting theory, where the decay rate of non-radiative modes is zero, such correlation function could in principle still relax to a steady state by dephasing of the different modes, constituting a continuum. In Fig. S.1 we show that nevertheless these fail to relax. An interesting question then is whether taking non-linearities into account, which can provide an effective lifetime for the non-radiative modes, allows these quantities to relax.

In DMFT/NCA we find that these quantities do relax and correspond to a smoothed version in frequency of those predicted by a non-interacting theory, as shown in Fig. S.1. Nevertheless, these predictions might be limited by inaccuracies of our approach in this regime (of the NCA). These results also show an example of quantities for which the predictions of the interacting theory in the weak-drive intensity limit  $\Omega/\Gamma \rightarrow 0$  might depart from those of the non-interacting theory. The local Green's functions from the non-interacting theory is also used to initialize the DMFT, by adding an artificial damping.

### Appendix C: Nonequilibrium steady-state DMFT

Here we present the self-consistency conditions for the DMFT approach for the steady state of the master equation (1). We refer to [42] for a detailed derivation.

DMFT maps the lattice model (1) onto an effective impurity model, describing a single site of the lattice coupled to an effective field, as in Gutzwiller mean-field, and

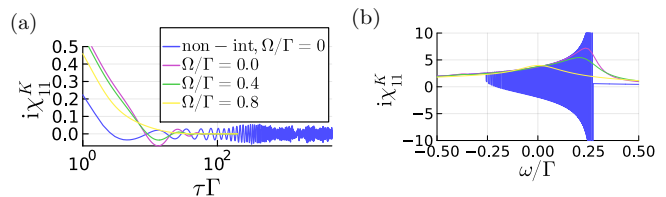


FIG. S.1. The local atomic Keldysh Green's function  $i\chi_{11}^K(\tau) = \lim_{t \rightarrow \infty} \langle \{ \sigma^-(t + \tau), \sigma^+(t) \} \rangle - \langle \sigma^-(t + \tau) \rangle \langle \sigma^+(t) \rangle$  computed from a non-interacting theory for  $\Omega \rightarrow 0$  and in DMFT in real time (a) and frequency (b), for the same parameters as in Fig. 2 (c).

to an effective environment. In the present case, the impurity model is a generalized spin-boson model, which in the steady state is described by the time-translation invariant Keldysh action

$$S^{\text{imp}} = S_0^i + \frac{1}{2} \int_{-\infty}^{\infty} dt \left[ \varsigma_i^\dagger(t) \tau_3 b + \text{hc} \right] - \frac{1}{2} \int_{-\infty}^{\infty} dt \int_{-\infty}^{\infty} dt' \varsigma_i^\dagger(t) \tau_3 \mathcal{W}(t - t') \tau_3 \varsigma_i(t') \quad (\text{C1})$$

Here  $\varsigma_i = (d_{i+}, \bar{d}_{i+}, d_{i-}, \bar{d}_{i-})^T$  is a vector in Nambu and Keldysh formalisms, where  $d = \langle \sigma^- \rangle$  and  $\bar{d} = \langle \sigma^+ \rangle$  are average values on spin coherent states [58], and the  $+$  and  $-$  indices indicate to which branch of the Keldysh double contour the fields belong to.  $b$  and  $\mathcal{W}$  represent the effective field and effective environment, which are site-independent for a homogeneous steady state.  $\tau_3$  is a diagonal matrix with entries  $(1, 1, -1, -1)$  arising in the Keldysh-Nambu formalism, where a Nambu formalism is needed to allow for nonzero values of the anomalous correlators  $\langle \sigma^\pm \sigma^\pm \rangle$ , which arise due to the drive term, breaking the  $U(1)$  symmetry of the undriven problem.

The self-consistent conditions correspond to a set of matrix relations in frequency and momentum space:

$$\Pi_{\text{loc}} = [\tau_3 \chi_{ii}^{-1} \tau_3 + \mathcal{W}]^{-1} \quad (\text{C2})$$

$$U_{ii} = \frac{1}{N} \sum_k [W_k^{-1} - \Pi_{\text{loc}}]^{-1} \quad (\text{C3})$$

$$\mathcal{W}^{-1} = \Pi_{\text{loc}} + U_{ii}^{-1} \quad (\text{C4})$$

$$b_\pm = (\mathcal{W}^R(\omega = 0) - W_{k=0}^R(\omega = 0)) \langle \varsigma_{i\pm} \rangle. \quad (\text{C5})$$

Here the superscript “ $R$ ” indicates the retarded component and  $b_\pm$  and  $\langle \varsigma_{i\pm} \rangle$  the  $+$  or  $-$  components of the corresponding vectors.  $W_k$  is a known matrix with entries defined by the Fourier transforms of (4) and (5)

$$\tau_3 W_k \tau_3 = \begin{pmatrix} V_k - \frac{i\Gamma_k}{2} & 0 & 0 & 0 \\ 0 & V_k - \frac{i\Gamma_k}{2} & 0 & i\Gamma_k \\ i\Gamma_k & 0 & -V_k - \frac{i\Gamma_k}{2} & 0 \\ 0 & 0 & 0 & -V_k - \frac{i\Gamma_k}{2} \end{pmatrix} \quad (\text{C6})$$

Assuming one can compute from the impurity action (C1) the local connected Green's function  $\chi_{ii}(\tau) = -i \lim_{t \rightarrow \infty} \langle \varsigma_i(t + \tau) \varsigma_i^\dagger(t) \rangle_{S_{\text{imp}}^{\text{con}}}$  and expectation value  $\langle \varsigma_i \rangle$ , then these equations determine  $\mathcal{W}, b, \Pi_{\text{loc}}$  and  $U_{ii}$ , such that the impurity problem represents the original lattice problem.

The connected propagator of the lattice  $\chi_{ij}(\tau) = -i \lim_{t \rightarrow \infty} \langle \varsigma_i(t + \tau) \varsigma_j^\dagger(t) \rangle^{\text{con}}$  can then be computed by  $\chi^{-1}(k, \omega) = \tau_3 (\Pi_{\text{loc}}^{-1}(\omega) - W_k) \tau_3$ .

We notice that this DMFT approach reduces to Gutzwiller mean-field theory fixing  $\mathcal{W}(\omega) = 1/N \sum_k W_k = W_{ii}$ .

#### Appendix D: Schemes for solving the DMFT equations

The usual procedure to solve the DMFT self-consistent equations is by a fixed-point iteration scheme. Here we go beyond this scheme and implement a gradient-based method. In the following, we first describe the fixed-point iteration scheme.

##### Fixed-point iteration scheme

Starting from a guess for  $b$  and  $\mathcal{W}$ , such as the mean field solution for the first and the single-atom decay for the second  $\mathcal{W} = 1/N \sum_k W_k$ , the following steps are iterated until a fixed point is reached:

- *Solving the impurity model:* given  $\mathcal{W}, b$ , the spin model is solved using the impurity solver, computing the steady state density matrix  $\rho_s$  and atomic correlation function  $\chi = \begin{pmatrix} \chi^{++} & \chi^{+-} \\ \chi^{-+} & \chi^{--} \end{pmatrix}$  for  $t > 0$ , where the entries are  $2 \times 2$  matrices in Nambu space. Then  $\chi$  at negative times  $t < 0$  is obtained assuming the steady state relation

$$\chi_{\alpha\beta}^{ab}(-t) = -[\chi_{\beta\bar{\alpha}}^{ba}]^*(t) \quad (\text{D1})$$

where the conjugate-transpose of both Nambu  $a, b$  and Keldysh  $\alpha\beta$  indices is taken and the Keldysh indices  $\alpha, \beta \in [+, -]$  are negated, such that  $\bar{\alpha} = -\alpha$ .

- *updating the Weiss field  $\mathcal{W}$  and effective field  $b$ :* we evaluate the self-consistent equations (C2),(C3),(C4) and (C5) where in frequency and momentum space inverses of Green's functions are simply given by a matrix inverse of their  $4 \times 4$  Nambu-Keldysh structure. These give new values for  $b$  and  $\mathcal{W}$ , which are transformed back into real time to iterate the procedure.

An important point of the update procedure concerns how to define the Green's functions at time  $t = 0$  such as to interface the NCA impurity solver and Keldysh

field theory. This is discussed in [42].

##### Linear-mixing and Broyden schemes

One DMFT step in a fixed-point iteration scheme can be considered as a functional  $G$  of the input hybridization function  $\mathcal{W}$  and effective field  $b$ , i.e.  $(\mathcal{W}^{\text{new}}, b^{\text{new}}) = G\{\mathcal{W}^{\text{old}}, b^{\text{old}}\}$ . This is iterated until a fixed point is reached. Defining a mapping  $F$  as the difference  $F\{\mathcal{W}, b\} = G\{\mathcal{W}, b\} - (\mathcal{W}, b)$  the approach to self-consistency clearly corresponds to solving the system of equations  $F\{\mathcal{W}, b\} = 0$ . A fixed point iteration scheme converges if all the eigenvalues of the linearization of  $G$  in the vicinity of the fixed point are strictly less than 1 in absolute value [53]. This might not be the case for all solutions of the DMFT equations  $F$  and a fixed-point iteration scheme might diverge despite these being physical solutions [53, 59]. In such cases, convergence can be achieved in some cases by a linear mixing scheme (see below), or by gradient-based methods that guarantee convergence to all solutions.

First let's consider the equation for  $b$ . If we keep  $\mathcal{W} = 1/N \sum_k W_k$  fixed, this corresponds to a Gutzwiller mean-field procedure. In this case we found that a fixed point iteration scheme only converges in the large-drive intensity phase, but not in the low-drive-intensity one, when the two are separated by a first order transition for  $k_0 a \lesssim 1$ . Therefore, we adopt a Newton method to determine  $b$ . The problem corresponds to finding the zero of the function  $\tilde{F}(b) = b - (\mathcal{W}^R(\omega = 0) - W_{k=0}^R(\omega = 0)) \langle \varsigma \rangle$  ((C5)). In a Newton method, the update is  $b_{\text{new}} = b_{\text{old}} - J^{-1}(b_{\text{old}}) \tilde{F}(b_{\text{old}})$ , where  $J$  is the Jacobian of  $\tilde{F}$ . To compute the Jacobian, we use the Kubo formula  $\langle \varsigma \rangle = -\chi^R(\omega = 0) \delta b$  relating the steady-state average values and the perturbation  $\delta b$  (the minus sign reflect that of  $b$  in the Hamiltonian), leading to  $J = \mathbb{1} + (\mathcal{W}^R(\omega = 0) - W_{k=0}^R(\omega = 0)) \chi^R(\omega = 0)$  (note that non-connected Green functions should be used instead of connected, but for the retarded component in the steady state these are the same).

Even with this improvement, we find that convergence of DMFT slows down as the drive intensity decreases, and below a certain intensity no solution is found. For this reason we went beyond the fixed point scheme also to determine the hybridization function  $\mathcal{W}(\omega)$ . A simple improvement is achieved by mixing the previous and new guesses for  $\mathcal{W}$ , indexed as  $m$  and  $m-1$ , in the fixed-point iteration scheme:

$$\mathcal{W}^{\text{input}, (m)} = \alpha \mathcal{W}^{\text{new}, (m)} + (1 - \alpha) \mathcal{W}^{\text{input}, (m-1)}$$

where  $\alpha \in [0, 1]$  is a mixing parameter. Unfortunately, there are situations where this simple linear mixing approach fails even for small values of  $\alpha$ . To exclude this possibility we also implemented a Broyden's method, as described in [53], that estimates the gradient in an iterative manner. This still depends on a parameter  $\alpha$ , corresponding to the linear mixing parameter, while other parameters are fixed as in [53].

In the present problem of the master equation (1) we

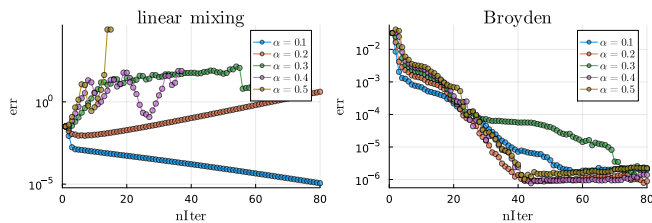


FIG. S.2. DMFT error as a function of number of DMFT iterations, starting close to the previously found solution at  $k_0 = 2$  and  $\Omega = 0.3, \Delta = 0$ . Here  $dt = 0.1$  and  $t_{\max} = 200$ .

find that using a linear mixing scheme with a small  $\alpha$  a solution is found up to smaller drive intensities with respect to a fixed-point iteration scheme. The Broyden's algorithm speeds up convergence, but at low enough drive intensities and small enough  $k_0 a$  also with this method no solution was found for our DMFT/NCA approach. This is both due to the emergence of non-uniform steady-states for some parameters (as discussed in the main text) and to the NCA becoming inaccurate far from the limit of independent atoms. An example of convergence in the low-drive regime is shown in Fig. S.2, where the DMFT error at the  $m$ -th iteration is defined as

$$e(m) = \max_{t_i, \eta, \zeta} (|[W_m(t_i)]^{\eta\zeta} - [W_{m-1}(t_i)]^{\eta\zeta}|) + \max_{\eta} (b_m^\eta - b_{m-1}^\eta) \quad (\text{D2})$$

where  $\eta, \zeta$  are Keldysh-Nambu indices. Using Broyden's scheme and in the low-drive regime the error saturates to a small (negligible) value, instead of decreasing monotonically, due to finite numerical accuracy (mainly related to finite timestep and momentum-integration errors). Also Fig. S.2 shows that a small mixing parameter  $\alpha$  is needed for convergence in the linear mixing procedure, while a larger one can be used with Broyden's algorithm.

### Appendix E: Exact limits of DMFT

Here we discuss two exact limits of DMFT in this context. The first is the limit of independent atoms, in which the impurity problem becomes equivalent to a single site of the original lattice problem (the impurity action (C1) reduces to a single-site action with  $b = 0$  and  $\mathcal{W} = 1/N \sum_k W_k$  describing the local dissipation). We note that in this limit the NCA solver used here exactly reduces to a Lindblad master equation, introducing no further approximations on the solution of the single-site problem.

Also, DMFT becomes exact when the model reduces to non-interacting bosons, such as in the limit of low drive intensity and in absence of dissipationless modes  $k_0 > k_0^{\max}$  (as discussed in Appendix B). Referring to its derivation in [42], we recall that DMFT solves a lattice problem equivalent to Eq. (1), in which auxiliary bosonic degrees of freedom are introduced decoupling the non-local terms with a Hubbard-Stratonovich transformation.

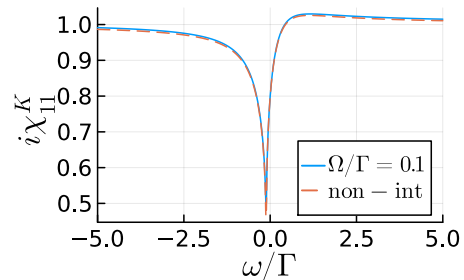


FIG. S.3. The local atomic Keldysh Green's function defined as in Fig. S.1 computed from a non-interacting theory for  $\Omega \rightarrow 0$  (dashed line) and in DMFT (solid), for  $k_0 a = \pi$  and  $\Delta = 0$ . This deviates from a Lorentzian shape for a single atom due the dipolar interactions between the atoms.

The resulting boson-atom lattice problem action reads  $S_{\text{HS}} = S_0 + S_{\phi\phi} + S_{\phi\sigma}$ , where  $S_0 = \sum_r S_{0,r}$  is the action of decoupled atoms at position  $r$ ,  $S_{\phi\phi}$  is a free-bosons action in terms of a Nambu vector of complex bosonic fields  $\phi_r$

$$S_{\phi\phi} = \frac{1}{2} \int_{-\infty}^{\infty} dt dt' \sum_{rr'} \phi_r^\dagger(t) \tau_3 [W^{-1}]_{rr'}(t-t') \tau_3 \phi_{r'}(t'),$$

and  $W_{rr'}(t-t')$  is the Fourier transform of (C6).  $S_{\phi\sigma}$  describes a *local* linear coupling term between bosons and atoms (with spin Nambu fields  $\varsigma$  defined as in (C1))

$$S_{\phi\sigma} = \frac{1}{2} \sum_r \int_{-\infty}^{\infty} dt \phi_r^\dagger(t) \tau_3 \varsigma_r(t) + \text{hc}$$

In the non-interacting limit, the atoms can be integrated out with a gaussian integral. This results into a self-energy for the auxiliary bosons which, importantly, is local in space  $\Pi_{rr'} = \Pi_{\text{loc}} \delta_{rr'}$ , as the atoms are only coupled to each other through the auxiliary bosons. Secondly, one can show that the boson-atom lattice model, being entirely quadratic, can be exactly mapped onto the impurity model (C1) with a cavity construction where all other sites are integrated out. Since these are the two assumptions on which DMFT rests [60, 61] this approach becomes exact in this non-interacting limit. In Fig. E we show that the local Green's functions computed within DMFT at low drive intensities and for large enough  $k_0 a$  agree with those computed from a non-interacting model. In Fig. S.1 instead we showed that at smaller values of  $k_0 a$  the two deviate as non-linear effects become important. We note though that the NCA used to solve the impurity problem introduces a further approximation, which is justified close to the limit of independent atoms where dipolar interactions are small enough. This eventually limits our DMFT/NCA approach in the low-drive-intensity and  $k_0 < k_0^{\max}$  regime in which dipolar interactions are strong and the atoms behave collectively.

### Appendix F: Linear stability equations

The homogeneous DMFT equation (C5) can be generalized to allow a momentum and frequency dependent effective field, while keeping the effective bath homogeneous, allowing to study the linear stability of such perturbations.

The field must then satisfy the self-consistent condition  $b_k(\omega) = [\mathcal{W}^R(\omega) - W_k^R(\omega)] \langle \varsigma_k(\omega) \rangle$  and, assuming a perturbation around a homogeneous value  $b_k(\omega) = b\delta(k)\delta(\omega) + \delta b_k(\omega)$ , the steady-state expectation  $\langle \varsigma_k(\omega) \rangle = \langle \varsigma \rangle \delta(k)\delta(\omega) + \langle \delta \varsigma_k(\omega) \rangle$  can be obtained from linear response  $\langle \delta \varsigma_k(\omega) \rangle = -\chi_k^R(\omega) \delta b_k(\omega)$ . Here “ $R$ ” in-

dicates the retarded components of  $\mathcal{W}$ , representing the effective environment,  $\chi$  is the local atomic Green’s function and  $W_k$  a matrix of the coherent and dissipative couplings (4) and (5) defined in Eq. (C6). Then a finite  $\delta b_k(\omega)$  can form if the following condition is satisfied:

$$\det \left\{ [W_k^R - \mathcal{W}^R(\omega)]^{-1} - \chi^R(\omega) \right\} = 0. \quad (\text{F1})$$

A similar equation determines the linear stability of a Gutzwiller mean-field theory by fixing  $\mathcal{W}(\omega) = 1/N \sum_k W_k$ .